Soft Matter

Post-synthesis modification of slide-ring gels for thermal and mechanical reconfiguration

Journal:	*Soft Matter*
Manuscript ID	SM-ART-12-2020-002260.R1
Article Type:	Paper
Date Submitted by the Author:	30-Mar-2021
Complete List of Authors:	Dikshit, Karan; University of Colorado Boulder, Materials Science and Engineering Program Bruns, Carson J.; University of Colorado Boulder, ATLAS Institute / Paul M. Rady Department of Mechanical Engineering

Soft Matter

ARTICLE TYPE

Cite this: DOI: 00.0000/xxxxxxxxxx

Post-synthesis modification of slide-ring gels for thermal and mechanical reconfiguration†

Karan Dikshit[a] and Carson J. Bruns*[b,c]

Received Date
Accepted Date

DOI: 00.0000/xxxxxxxxxx

Ring-sliding behavior in polyrotaxanes imbues gels, elastomers, and glasses with remarkable stress-dissipation and actuation properties. Since these properties can be modulated and tuned by structural parameters, many efforts have been devoted to developing synthetic protocols that define the structures and properties of slide-ring materials. We introduce post-synthetic modifications of slide-ring gels derived from unmodified α-cyclodextrin and poly(ethylene glycol) polyrotaxanes that enable (i) actuation and control of the thermo-responsive lower critical solution temperature (LCST) behavior of ring-modified slide-ring hydrogels, and (ii) chemically bonding separate gels into hybrid or shape-reconfigured macro-structures with a slide-ring adhesive solution. The mechanical properties of the post-modified gels have been characterized by shear rheology and uniaxial tensile tests, while the corresponding xerogels were characterized by wide-angle X-ray scattering. These demonstrations show that post-synthetic modification offers a practical solution for re-configuring the properties and shapes of slide-ring gels.

1 Introduction

Polyrotaxanes (PRs) are mechanically bonded macromolecules with threaded ring-on-string structures that often confer advantageous properties to materials because their ring-sliding motions offer mechanisms for both stress dissipation[1–4] and actuation.[5–14] In particular, Harada's discovery[15,16] of inclusion complexes of poly(ethylene glycol) [PEG] in α-cyclodextrin [α-CD] enabled the synthesis[17] of PEG$\subset$ (α-CD)$_n$ PRs, which are appealing because they can be made from low-cost, non-toxic, commercially available compounds in reasonably high yield. PEG$\subset\alpha$-CD PRs have been utilized in a wide range of functional materials, including elastic binders for battery electrodes,[18–20] polymer electrolyte gels[21,22] and solids,[23–25] shape-changing 3D-printed monoliths,[26–28] self-healing materials,[29] abrasion-resistant coatings,[30] high-damping rubbers,[31,32] ductile glasses,[33–36] pressure-responsive[37] and gas separation[38] membranes, multivalent inhibitors for cellular processes,[39–41] dynamic surfaces for directing cell behavior,[42–46] imaging/contrast agents,[47] as well as drug,[48–57] gene[58–68] and enzyme[69,70] delivery vehicles.

In this work we focus on solvated PR networks known[1] as slide-ring (SR) gels. These gels embody aspects of the slip-link model that was developed by Ball *et al.* to describe the viscoelastic behavior of entangled polymers,[71] as well as the sliding gels concept proposed by de Gennes[72] to model polymer chains translating through ion-bridge crosslinks without losing contact. By crosslinking the mobile α-CD rings of PRs, Okumura and Ito[1] introduced the first true ring-sliding gels two decades ago. Under deformation, the sliding motions of the chains through the rings, known as the pulley effect,[73] enhances the extensibility and toughness of the gels. The entropy of mobile CD rings between the junctions likely also contribute to their mechanics.[74–78] However, SR gels show a number of anomalous behaviors compared to chemical gels, which are not yet fully understood, including (i) high softness,[2] with a reduced dependence of modulus on crosslink density,[79,80] (ii) strain-hardening behavior without hysteresis in stress-strain curves,[73] counter to the slip-link model, (iii) suppressed stretching-induced swelling,[81] (iv) reduced strain coupling in multiaxial tension,[82] (v) two plateaus of viscoelastic relaxation, indicating a dynamic transition between rubbery and ring-sliding states[75,83], and (vi) high fracture and crack propagation resistance.[84–86] Since their crosslinks can translate without dissociating, but only until further sliding is blocked by stoppers, SR gels are conceptually in between physical and chemical gels. Like physical gels, the "stored" length of the polymer chains is consumed completely as SR gels are strained. Like chemical gels, SR gels are capable of elastic recovery at high strains.

[a] *Materials Science and Engineering program, University of Colorado Boulder, Boulder, Colorado 80309, USA*
[b] *ATLAS Institute, University of Colorado Boulder, Boulder, Colorado 80309, USA*
[c] *Paul M. Rady Department of Mechanical Engineering, University of Colorado Boulder, Boulder, Colorado 80309, USA. Email: Carson.Bruns@colorado.edu*
† Electronic Supplementary Information (ESI) available at DOI: 10.1039/cXsm00000x/

The promising mechanical properties of slide-ring materials motivates further exploration in the domain of hydrogels, which are often used in contact lenses, wound dressings, hygiene products, tissue engineering matrices, and drug delivery.[87] However, SR hydrogels based on α-CD:PEG PRs are less accessible than the corresponding organogels because neutral-pH water is a poor solvent that promotes α-CD aggregation and deactivates the pulley effect.[88–90] This aqueous incompatibility, which limits potential biomedical applications of slide-ring mechanics, may be addressed by synthetic modification of the PR scaffold. The solubility of α-CD:PEG PRs can be tuned with various stoppers,[48,50,55,91–93] or by direct functionalization of the α-CD rings with a variety of reactions, including (i) ether formation using epoxides such as propylene oxide (hydroxypropylation)[94] and other glycidic reagents,[95,96] (ii) esterification with acyl halides,[10,97–99] anhydrides,[97] carbonylimidazoles,[8,80,100,101] or ring-opening reagents such as succinic anhydride[102] and ε-caprolactone,[103] (iii) urethane formation mediated by carbonyldiimidazole[104] or isocyanates,[105] (iv) oxidation,[106] (v) silylation,[107] (vi) alkylation by nucleophilic substitution,[96,107] (vii) ring-opening sulfoalkylation by sultones,[108] and (viii) nucleophilic addition.[109] Other modification chemistries, such as click reactions,[110] can be implemented by threading the PEG chains with pre-modified CDs during PR synthesis. Most SR hydrogels based on PEG$\subset\alpha$-CD PRs have been obtained after ring modifications such as acrylic,[3,12,105,111,112] amino acid,[113] and hydroxypropyl[29,85,114] grafts.

We envision an alternative approach to obtaining slide-ring hydrogels by modifying the α-CD rings of pre-formed organogels and exchanging solvents. Post-synthetic modifications of slide-ring gels are uncommon, but have included photo-isomerization of appended azobenzene units,[10] etching of interstitial colloidal silica templates,[115] surface oxidation by plasma treatment,[116] and nucleophilic substitutions at unreacted sites of cyanuric chloride-based crosslinks.[88,108] Post-synthetic chemical functionalization of the α-CD rings in SR gels remains an untapped opportunity. Other potential advantages of post-gel modifications include (i) the ability to generate a series of gels with systematically varied functional group coverage at identical crosslink densities (challenging to achieve from pre-modified PRs because the number hydroxyl sites available for crosslinking changes with increasing modification), (ii) simplified separation of unused reactants or waste products through solvent washing (no dialysis, lyophilization, or precipitation required), and (iii) the opportunity to bond separate gels together. In order to showcase these benefits, we demonstrate two post-synthesis modifications of PR gels. First, we show that post-synthesis acetylation allows us to control the swelling, thermal response, transparency, and mechanical properties of slide-ring hydrogels with varying modification ratios. Second, we demonstrate a "cut-and-paste" modification that bonds macroscopic gels together, allowing them to be reconfigured into structures with spatially segregated domains of functionalization, or complex shapes that would be unobtainable in conventional molds. We have characterized the mechanical properties of these gels using shear rheology and tensile tests. We show that post-synthesis modification is a practical way to introduce shape change, either by thermal actuation above and below the LCST, or by cut-and-paste mechanical reconfiguration of SR gels.

2 Experiments

Materials. 35 kDa molecular weight (MW) poly(ethylene glycol) [PEG35k] (EMD Millipore Corporation), (2,2,6,6-tetramethylpiperidin-1-yl)oxyl [TEMPO], 1-adamantanamine hydrochloride [$AdNH_2$·HCl], and 270 kDa MW pullulan [PL] (TCI Chemicals, Japan), α-cyclodextrin [α-CD], (benzotriazol-1-yloxytris(dimethylamino)phosphonium hexafluorophosphate) [BOP] reagent (Chem Impex International, Inc.), ethylene diisopropylamine [EDIPA] (Alfa Aesar), carbonyldiimidazole [CDI], sodium hypochlorite [NaOCl] solution with 5% free chlorine (Spectrum Chemicals, USA), sodium bromide [NaBr] (Acros Organics), hydrochloric acid [HCl] (37%, Sigma-Aldrich), sodium hydroxide [NaOH], lithium chloride [LiCl], acetic anhydride [Ac_2O], *N,N*-dimethylaminopyridine [DMAP], pyridine, dichloromethane [DCM], dimethylformamide [DMF], dimethyl sulfoxide [DMSO] (Fisher Chemicals, USA), ethanol [EtOH] and methanol [MeOH] (Decon Laboratories, Inc.), were used as received. Reverse osmosis (RO)-purified water was obtained from a centralized source in our campus facility through a tap.

Synthesis of unmodified polyrotaxane (uPR). Adamantane (Ad)-capped unmodified polyrotaxane (uPR) was synthesized from poly(ethylene glycol)dicarboxylate (PEGDC), α-CD, and adamantamine [$AdNH_2$] using a modified literature protocol.[117]

PEGDC. PEG35k (10g, 0.3 mmol) was dissolved in RO water (100 mL) maintained at pH 10 with 1 M NaOH solution (100 μL). TEMPO (100 mg, 0.6 mmol), NaBr (100 mg, 1 mmol), and NaOCl solution (15 mL) were added and the reaction was stirred at room temperature (RT) for 20 min. EtOH/MeOH, equal in amount to NaOCl solution, was added to quench any unreacted NaOCl, followed by dropwise addition of HCl (0.003 M) until the pH was <2, in order to ensure protonation of PEGDC. The polymer was extracted from the aqueous solution into DCM (over 3 aliquots of 100 mL each), dried in a rotary evaporator, and residue was dissolved in hot EtOH (200 mL) followed by overnight refrigeration to precipitate PEGDC. The product was collected by vacuum filtration and dried under vacuum at 60 °C to yield PEGDC (7.2 g, 72%) as a white powder, which was used without further purification.

uPR. PEGDC (3g, 0.09 mmol) was dissolved in RO water (100 mL) and maintained at 80 °C with stirring. α-CD (12g, 12 mmol) was added and the solution was stirred for 30 min until it was no longer turbid. The solution was placed in a refrigerator at 4 °C overnight to precipitate the PEG$\subset$ $(\alpha\text{-CD})_n$ inclusion complex, or pseudo-polyrotaxane (pseudoPR), which was isolated as a white powder by lyophilization and used without further purification. The crude pseudoPR ($\sim$13 g) was dispersed in anhydrous DMF (100 mL). BOP reagent (0.48g, 1.1 mmol), $AdNH_2$ (1.6g, 1.1 mmol) – obtained from [$AdNH_2$·HCl] by washing with aqueous NaOH, extraction in DCM, and drying by rotary evaporation – and EDIPA (200 μl, 1.1 mmol) were added to the slurry and the mixture was stirred at RT for 30 min. The slurry was placed in a refrigerator at 4 °C overnight to stopper the pseudoPR, affording

the crude unmodified polyrotaxane (uPR). The resulting polymer was purified by multiple steps of centrifugation, first with water, then with methanol. The product was dried under vacuum at 70 °C overnight. The residue was dissolved in DMSO at a concentration of 10% w/v, and the centrifugation and drying procedure was repeated a second time to obtain uPR as a white solid (7.9 g, 68%). The ^{1}H NMR spectrum of uPR, consistent with literature,[117] was used to estimate an inclusion ratio of ∼30% (corresponding to approximately 120 α-CD rings per chain) by comparative signal integration of the Ad and α-CD resonances (Fig S1).† The molecular weight (MW) of uPR is therefore estimated by ^{1}H NMR spectroscopy to be ∼152 kDa, which is in reasonable agreement with our MW estimation of ∼164 kDa by gel permeation chromatography (GPC, Fig. S2).†

Formation of unmodified slide-ring gel (SRG0) and pullulan gel (PLG0). uPR (100 mg, 0.8 μmol) or pullulan (100 mg, 0.4μmol) was dissolved in a solution of LiCl (80 mg, 2 mmol) in DMF (1 mL), which is known[97] as a good solvent for uPR. CDI (35 mg, 0.2 mmol) was added to the solution and vortexed for 30 s to form the pre-gel solution, which was cast in a 20 ml glass scintillation vial, capped, and placed on a leveled glass plate in an oven at 60 °C. After 24 h, the vials were cooled to RT and the corresponding organogels were extracted as transparent discs upon breaking open the glass vials. The initial sizes of the gel discs were approximately 25 mm in diameter and 1.25 mm in height. The slide-ring gel (SRG0) or pullulan gel (PLG0) discs were placed in 250 mL glass jars to swell with an excess of LiCl/DMF solution (8% w/v). The LiCl/DMF solution was decanted and replenished twice over a 24 h period while being gently agitated on an orbital shaker at 60 rpm to remove impurities from the swollen gels.

Post-Synthetic acetylation of SRG0 and PLG0. Pyridine (500 μL, 6 mmol) and DMAP (100mg, 0.8 mmol) were added to a LiCl/DMF solution (8% w/v, 20mL) containing a complete swollen disc of SRG0 or PLG0 (100 mg with respect to the parent polymer) in a 250 mL glass jar. After 2 hours of agitation at room temperature on an orbital shaker (60 rpm), Ac_2O was added at varying concentrations (150-650 mM, Scheme 1) and the reaction continued with orbital shaking for 24 h. The gel was purified by multiple washings with an excess of LiCl/DMF solution, decanting and replenishing with fresh washing solution twice a day for at least 48 h to obtain the modified organogels SRG1–SRG3 or PLG1–PLG3.

Preparation of hydrogels. The organogels SRG0–SRG3 or PLG0–PLG3 were transferred to a bath of RO water, which was decanted and refilled with fresh RO water twice a day for at least 48 h with continuous orbital shaking to obtain the corresponding hydrogels.

Preparation of xerogels. SRG0–SRG3 hydrogels were cut into 5-mm circular pieces at RT, quick-frozen with liquid N_2, and freeze-dried in a lyophilizer for 48 h. A second set of slide-ring xerogels were prepared from high-temperature SRG0–SRG3 hydrogels by drying at 70 °C in an oven for 48 h. The volume changes of the xerogels were estimated by measuring the height and diameter of the discs with calipers before and after the drying procedure (Table S1).†

Gel cut-and-paste procedure. Pieces of SRG0–SRG3 or PLG0–

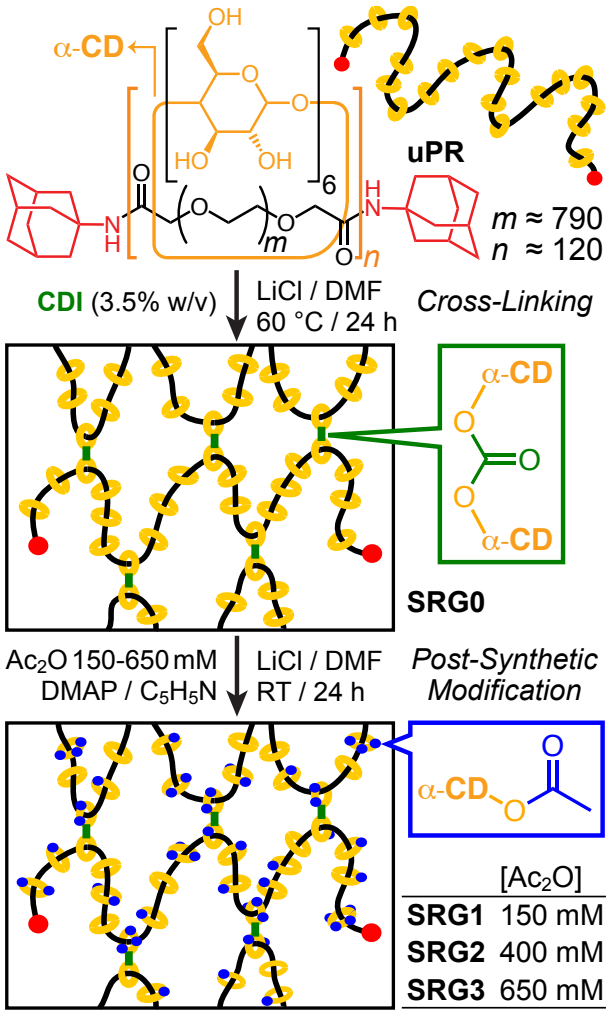

Scheme 1 Synthesis and post-synthetic modification of slide-ring gels

PLG3 organogels were pre-arranged into the desired structural forms with "joints" where the edges to be bonded were in close contact. The joints were bonded together by application of either slide-ring adhesive (SRGlue) or pullulan adhesive (PLGlue), each consisting of a 10% w/v pregel solution (10 μL) of uPR (for SRGlue) or PL (for PLGlue) and HMDI (3.5%) in DMSO, until the joint gap was filled. These glued assemblies were transferred into an oven maintained at 60 °C to cure the adhesive. After 6 h, the bonded assembly was transferred into a bath of excess DMSO or water and equilibrated at RT for 48 h with occasional solvent replacement to remove unreacted impurities from the gels.

Characterization Techniques. Nuclear Magnetic Resonance (NMR) spectroscopy was performed on a Varian 400 MHz NMR spectrometer. X-ray scattering experiments were performed using Forvis Technologies wide-angle X-ray scattering (WAXS) 30 W Xenocs Genix3D X-ray source (Cu anode, wavelength λ = 1.54 Å) and Dectris Eiger R 1 M detector. The data were collected at a sample-to-detector distance of 168.97 mm, while the samples were exposed to X-rays for 30 minutes. Photographic evidence was acquired with a 16 MP Sony IMX 159 camera after equilibrating the hydrogels in baths at temperatures of 25°C, 35 °C, 50°C, 60°C, and 70°C, maintained by a temperature-controlled

heating plate (Instec STC 200) for approximately 30 s before being transferred to a grid for immediate photo capture. ImageJ software (National Institute of Health, USA) was used to measure the cross-sectional area of photographed samples and quantify the observed shape changes in response to thermal stimuli. The 5-mm sections of a background grid are used to define the length scale of a pixel in the digital image, then the edges of gel are outlined manually and the number of pixels contained within the outline are converted into an area in mm^2.

Rheometry of SR and PL gels was carried out using a shear rheometer (Anton Paar MCR 301) equipped with a 8mm parallel plate geometry and an accompanying peltier plate for temperature control, which serves as the bottom plate. Dynamic oscillatory shear experiments were used to characterize viscoelasticity of the gels, using a nominal normal force of approximately 0.1 N and a gap varying between 0.6–1.4 mm, depending on the gel thickness. Mechanical spectra were recorded by performing frequency sweep, in the range of 0.1-628 rad/s, at a strain of 0.05%. This strain was confirmed to be in the linear viscoelastic regime by an amplitude sweep (Figure S3), varying from 0.01–10%, carried out at a frequency of 1 rad/s.† Temperature sweeps between 25–70 °C, were carried out at a frequency of 1 rad/s and a heating rate of 5 °C/min with a constant strain of 0.05%. We employed the Anton Paar TruGap^{TM} setting to maintain a fixed gap size during temperature sweeps, which ensures that thermal volume changes in the apparatus are accounted for in dynamic mechanical testing. Uniaxial pulling tests to determine gel adhesion efficiency were carried out using a Q800 dynamic mechanical analyzer (TA Instruments).

3 Results and discussion

Modification of PEG⊂α-CD PRs with hydrophobic functional groups such as Me and Ac can improve their water solubility by weakening the multivalent hydrogen bonding interactions between α-CD rings; these PRs tend to exhibit a lower critical solution temperature (LCST) and crash out of water when heated.[118–122] LCST behavior is a well-understood phenomenon that is often leveraged for thermo-responsive polymer actuators, especially those based on poly(*N*-isopropyl)acrylamide[123] (pNIPAAM). While these materials can suffer from brittle mechanics and slow deswelling kinetics, pNIPAAM-grafted PR hydrogels are relatively tough and fast actuators, owing to their ring-sliding motions.[12,105] While the LCSTs of these copolymer hydrogels are dominated by pNIPAAM, we reasoned that SR hydrogels displaying small hydrophobic functional groups may also show LCST behavior, akin to their analogous PRs in water. Indeed, Lin *et al.* have recently shown that the α-CD rings of poly(acrylic acid)/PR copolymer hydrogels (without sliding crosslinks) can be methylated to achieve thermo-responsive shape change in 3D-printed monoliths.[28] Inspired by this work and that of Tamura and coworkers,[121,122] which showed varying LCST and aggregation behavior for aqueous acetylated PR (AcPR) compounds, we hypothesized that the thermo-responsive aggregation of CD rings could be controlled by the degree of acetylation in post-synthetically modified SR hydrogels.

We sought a series of SR gels with systematically varied acetylation ratios at fixed crosslink density, in order or to isolate the role of functional group coverage on the SR gel properties. We recognized that maintaining a fixed crosslink density in gels derived from a series of AcPRs with increasing Ac content would be challenging, since the number α-CD hydroxyl sites available for crosslinking decreases with increasing acetylation. Therefore, we chose instead to form (Scheme 1) a series of identical SR organogels (SRG0) from unmodified PR (uPR) with carbonyl crosslinks derived from CDI, and then systematically functionalize them post-gelation with Ac_2O. The SRG0 gels were swelled at RT in LiCl/DMF solution (8% w/v) for 24 h in the presence of DMAP, pyridine, and varying concentrations of Ac_2O (150-650 mM, Scheme 1) to afford SRG1–SRG3. Upon washing and exchanging into water, the sparsely acetylated SRG1 hydrogel was more transparent than the corresponding SRG0 hydrogel,

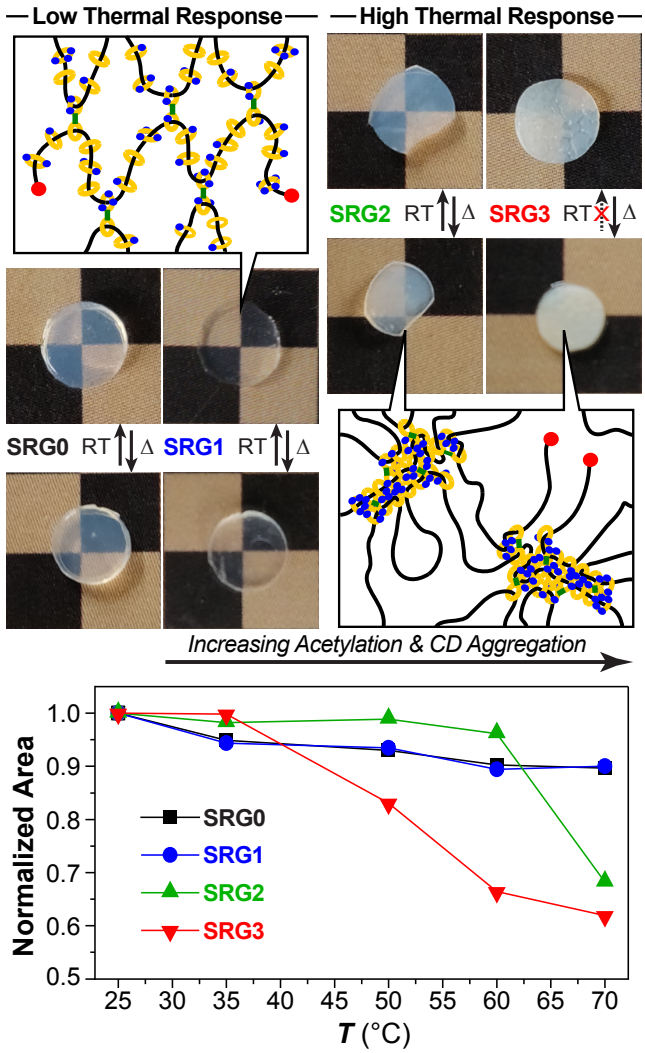

Fig. 1 Thermo-responsive behavior of unmodified hydrogel SRG0 and post-synthetically acetylated hydrogels SRG1–SRG3. While a small amount of acetylation enhances the transparency and swelling of hydrogel SRG1, heat-induced volume reductions and turbidity increase at higher acetylation ratios, until the thermo-responsive deswelling becomes irreversible in SRG3. The black and brown squares in the photographs are each 5x5 mm.

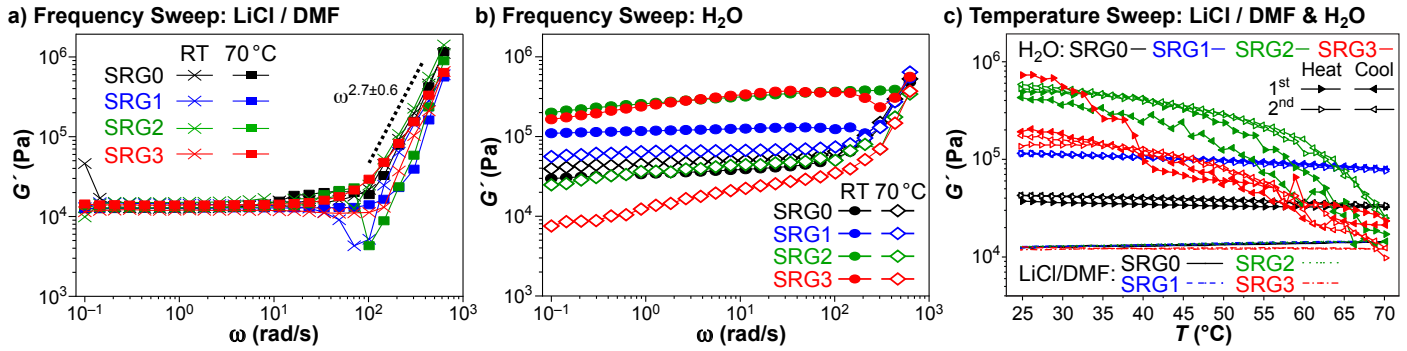

Fig. 2 Rheology of SRG0–SRG3. (a) Frequency sweeps in LiCl / DMF solution at RT and 70 °C. (b) Frequency sweeps in H_2O at RT and 70 °C. (c) Temperature sweeps in LiCl/DMF and H_2O at 1 rad/s. All measurements were performed in the linear viscoelastic regime at a strain of 0.05%.

while the more acetylated SRG2 and SRG3 gels were increasingly cloudy (Figure 1). The turbidity of the gels arise from the scattering of microscopic α-CD aggregates that form in water for both unmodified[88–90] and more highly acetylated SRGs, consistent with the behavior of the corresponding free AcPRs in water.[121,122] In accordance with prior works,[2,29,84,86,111] we also prepared a series of pullulan (PL) organogels and hydrogels analogously in order to compare the behavior in gels with sliding *versus* fixed crosslinks.

We investigated the response of hydrogels SRG0–SRG3 to changes in temperature. Photographs of the gels, cut into 5-mm discs and immersed in water at RT and 70 °C show (Figure 1) an increasing volume reduction with increasing acetylation. We plotted (Figure 1) the normalized cross-sectional areas of the SRG0–SRG3 discs as a function of temperature, based on digital image analysis of photographs recorded after 30 s of gel immersion in temperature-controlled water baths. The unmodified SRG0 and sparsely acetylated SRG1 show minimal size reductions of 10% each between 25–70 °C, whereas the cross-sectional areas of the more highly acetylated SRG2 and SRG3 are reduced by >30% over the same temperature range. The intermediate gel SRG2 exhibits a relatively sharp, reversible transition, with 90% of its total size reduction of 32% occurring between 60–70 °C. By contrast, the highly acetylated SRG3 shrinks more gradually by a factor of 38%, with a nearly linear dependence of size on temperature from 35–70 °C. With the exception of SRG3, the gels return to their original size within 2 minutes of equilibration in water at RT. SRG3 does not re-swell, indicating a critical acetylation ratio beyond which the gel collapses irreversibly as it is heated in water.

We turned to shear rheology to characterize how the mechanical properties of the slide-ring gels change with post-synthetic modification, solvent exchange, and heating (Figure 2). Beginning with the seminal work of Okumura and Ito,[1] rheological studies have been, and continue to be, a critical component of research on slide-ring materials.[73,75,76,79–83] Much of this work has relied on dynamic mechanical analyzers (DMAs) that perform oscillatory measurements in uniaxial tension. While DMAs are advantageous for reaching high strains, they are more limited in sample thickness and the potential for sample dehydration. Fewer SRGs have been characterized by shear rheology,[1,124] which is more strain-limited, but lowers dehydration risk (especially with a ring of mineral oil around the edges of a hydrogel) and allows for thicker samples.

A characteristic feature of SRGs in uniaxial frequency sweeps is the presence of two modulus plateaus—a low-frequency "sliding" plateau and a high-frequency rubbery plateau—with a transient response between them.[75,76,83] A shear frequency sweep (Figure 2a) of organogels SRG0–SRG3 in LiCl/DMF solution reveals that the storage modulus, G', is independent of deformation rate (angular frequency, ω) at low frequencies, and transitions to the transient state above 100 rad/s. The overlaid frequency sweeps of the organogels at RT and 70 °C show that they are also relatively insensitive to temperature changes, consistent with prior findings on SR organogels.[76] Unlike the DMA studies,[75,76,83] our sheared gels have not yet reached a rubbery plateau modulus at the upper frequency limit (628 rad/s) of the rheometer. In the high-frequency regime, the shear modulus of these gels scale as $G' \sim \omega^{2.7 \pm 0.6}$, which is significantly higher than that observed ($\omega^{2.0 \pm 0.2}$) for the analogous pullulan gels (Figure S4).† This scaling also exceeds those observed in DMA frequency sweeps of HMDI-crosslinked DMSO organogels derived from uPR reported in the literature,[75,76] which we analyzed with Plot Digitizer software[125] to determine a power law relationship of $G' \sim \omega^{0.7}$ in this transient region. The finding that our CDI-crosslinked organogels in LiCl/DMF stiffen more sharply when sheared in frequency sweeps suggests that solvent, crosslinker, sample geometry, and/or deformation mode may significantly alter the slide-ring mechanics, calling for future work to deconvolute the impact of these different factors.

When the SR organogels are exchanged into water, the corresponding hydrogels exhibit stark differences in rheology (Figure 2b-c), where G' increases with increasing acetylation. The low- and high-temperature frequency sweeps (Figure 2b) become more disparate at higher acetylation ratios. The moduli are more sensitive to frequency, except in the case of the well-solvated SRG1 at RT. The heated gels exhibit softening, except for SRG0, which hardens slightly at higher temperature. The transient regime is also pushed to higher frequencies, but is not observed in RT samples of SRG2 and SRG3, suggesting that they may already be in a rubbery state with deactivated ring-sliding pulley effect on account of α-CD aggregation.[88–90] For the sake

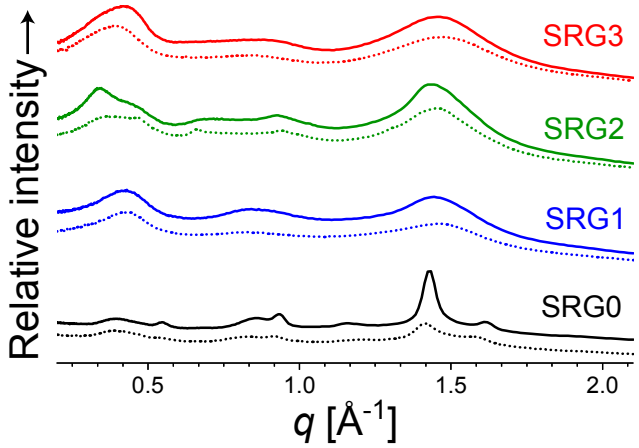

Fig. 3 Wide-angle X-ray scattering (WAXS) data of SRG0–SRG3 xerogels, obtained under different drying conditions. The dashed lines indicate xerogels obtained by freeze-drying a gel initially held at room temperature, while solid lines indicate xerogels obtained by dehydration of gels held at 70 °C.

of comparison, we also performed frequency sweeps on pullulan gels PLG0-PLG3 (Figure S4).† While these fixed-crosslink gels are stiffer than the slide-ring gels,[2] they show similar rheological behavior and also become more temperature-sensitive with increasing acetylation, indicating that our post-gelation modification procedure can be generalized to other types of gels.

In the temperature sweeps (Figure 2c), all four slide-ring organogels show almost identical behavior, with slight, almost negligible hardening at higher temperatures. In water, SRG0 and SRG1 show only mild, reversible softening as they are heated, while the more highly acetylated SGR2 and SGR3 hydrogels display severe drops in modulus at higher temperatures. This behavior is likely caused by the excluded water driven off by α-CD aggregation; similar softening above the LCST in physical/chemical hybrid pNIPAAM hydrogels has been attributed to the decreased volume fraction of microgel domains.[126] In the cooling cycle, SRG2 recovers its original modulus (with modest hysteresis), while SRG3 does not recover below temperatures of 40 °C, where the cooling curve becomes flat, consistent with its observed irreversible volume change. The temperature sweep data may be used as a secondary metric for the LCST, since the *G' vs. T* profiles are similar to the *Area vs. T* profiles plotted in Figure 1. We performed a second heat-cool cycle on the hydrogels to examine their reversibility. After an equilibration period of 20 h, SRG2 recovers its original profile with less hysteresis, whereas the irreversible gel SRG3 does not recover, with its modulus re-tracing that of the initial cooling cycle in both directions. After only 1 hour of equilibration, SRG2 transitions at a much lower temperature (Figure S5),† suggesting that its temperature-dependent microstructure recovers more slowly than its macroscopic shape.

Wide-angle X-ray scattering (WAXS) experiments were performed to interrogate the microstructural changes occurring in the gels. WAXS has been employed previously to characterize CD aggregation in modified polyrotaxanes, which tend to favor a hexagonal lattice of channel-type structures.[17,120,127] Lin *et al.* compared the XRD of xerogels obtained from thermo-responsive PR hydrogels at low and high temperatures, finding that the peak near $q = 0.5$ Å^{-1} intensifies with increasing levels of PR methylation.[28] Kato *et al.* found that the same signal shifts to higher q values, indicating a reduced distance between rings in amorphous samples of acetylated α-CD.[127]

Although the xerogel structure may not necessarily capture that of the hydrogel, we investigated the temperature-dependent effect of acetylation on xerogels by comparing (Figure 3) the WAXS profiles of xerogels obtained from freeze-dried and heat-dried hydrogels of SRG0–SRG3. The peak position at $q = 1.42$ Å^{-1}, attributed to the α-CD cavity, is consistent across all samples. In unmodified SRG0, the scattering signals are more numerous, intense, and sharp in the heat-dried samples than the freeze-dried samples, showing a pattern matching the hexagonally packed hydrogen-bonded CD channels observed in prior work.[17,120,127] The heat-drying process likely facilitates crystallization by allowing the gel to become more concentrated in solution, rather than while frozen in the solid state during freeze drying; in agreement, we observed (Table S1) that heat-dried samples undergo larger volume reductions than freeze-dried samples.† In all three acetylated gels, the steric interference on crystalline packing with increasing acetylation is evident in the broadening of signals, with amorphous halos replacing the peaks at $q = 1.62$, 0.92, and 0.55 Å^{-1} in SRG0. Acetylation also increases the peak intensities below $q = 0.5$ Å^{-1}, revealing a higher content of α-CD aggregates. It is noteworthy, therefore, that the WAXS profile of SRG1 is nearly identical when it is freeze-dried and heat-dried, whereas SRG2 and SRG3 show more differences in their freeze- and heat-dried scattering profiles. In SRG2, heat drying produces a strong signal at $q = 0.34$ Å^{-1}, suggesting an increase in ordered α-CD packing, but at a greater ring-to-ring distance than typically observed in hexagonal-packed α-CD cylinders, which are also present as indicated by the shoulder trailing this peak at $q = 0.46$ Å^{-1}. In SRG3, the low-q signal shifts to 0.44 Å^{-1} when heat dried, indicating a closer packing of acetylated α-CDs. Since freeze- and heat-dried SRG2 and SRG3 xerogels show more differences than those of SRG1, consistent with the solution-state behavior of the hydrogels, we reason that the microstructure of the hydrogel influences the microstructure of the xerogel as it is dried.

Recognizing that slide-ring organogels are amenable to post-synthesis modification, we speculated that their reactivity could be exploited at their surfaces to bond separate gels together. We formulated a "slide-ring adhesive" (Figure 4) comprising a pre-gel solution of uPR (10% w/v) and bis-isocyanate crosslinker HMDI (3.5% w/v) in DMSO. The freshly prepared solution is sufficiently viscous to occupy a gap space of <1 mm between two gel pieces obtained by cutting in half a dogbone sample designed for tensile testing (Figure 4a). Heating the slide-ring adhesive in an oven at 60 °C creates a bond at the interface of the two gel surfaces, although the gap remains visible. We created an analogous pullulan adhesive (PLGlue) that can also be used to bond slide-ring or pullulan gels by the same procedure.

We distinguish our "cut-and-paste" approach from "healing", where dynamic bond-breaking and bond-making reactions repair a gel network.[128] While a variety of gel-healing protocols

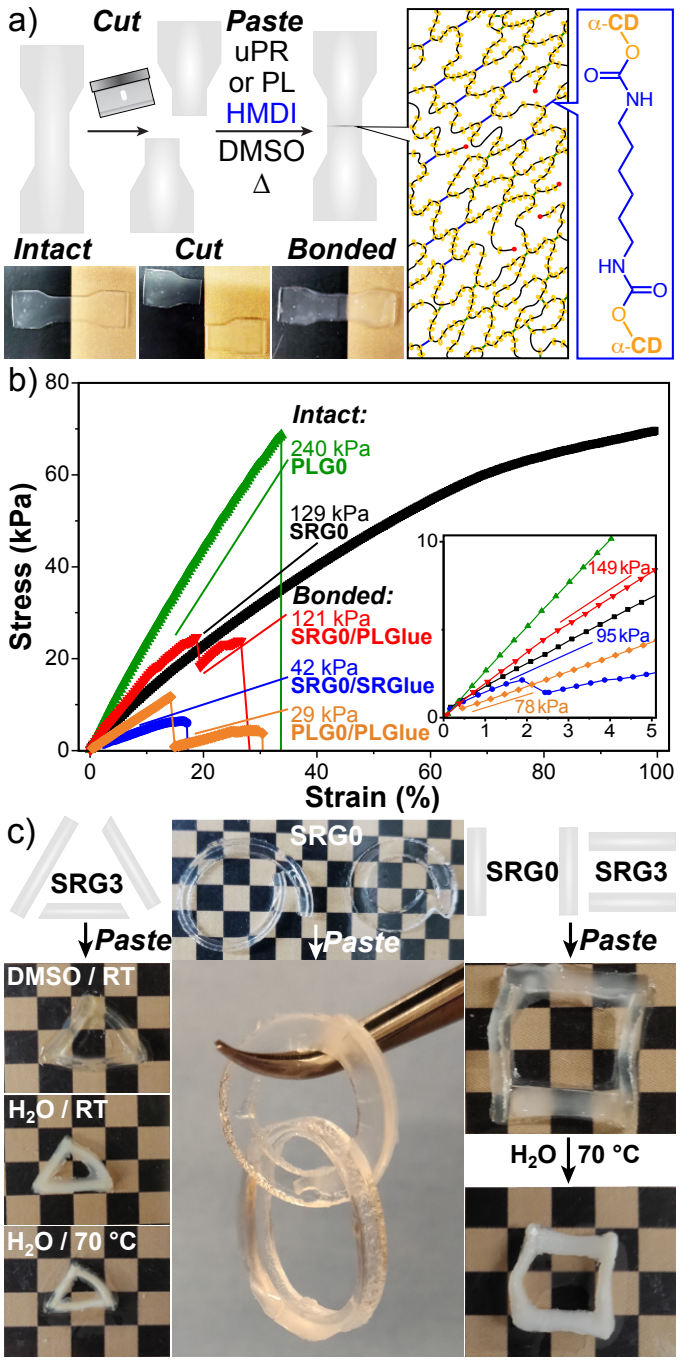

Fig. 4 Cut-and-paste post-gel modifications. (a) Procedure for cutting and re-bonding a dogbone organogel with a heated slide-ring adhesive (SRGlue) solution of uPR / HMDI or a pullulan adhesive (PLGlue) solution of PL /HMDI in DMSO. (b) Tensile tests comparing stress vs. strain in intact and bonded SRG0 and PLG0 dogbone samples with slide-ring adhesive (SRGlue) and pullulan adhesive (PLGlue). The inset magnifies the data in the low-strain region. (c) Photographic examples of SR gels reconfigured by the cut-and-paste approach with SRGlue, showing their stability to thermally triggered volume reduction (left), shape reconfiguration into topological links (center) and hybrid structures derived from different gel formulations (right).

have been reported,[129,130] including for slide-ring gels,[29] their requirement of reversible, dynamic bonds limits their applicability to gels such as SRG0–SRG3 and PLG0–PLG3, which do not have crosslinks amenable to bond scrambling. This irreversible cut-and-paste approach is appropriate for adhering slide-ring gels lacking these self-healing modalities, but it does not restore the network to its original state. Tensile tests of unmodified slide-ring and pullulan gels SRG0 and PLG0, respectively, are compared in the intact and bonded forms in Figure 4b. Consistent with previous findings,[2] the slide-ring gel is much softer and tougher than the pullulan gel at the same crosslinker concentration; the Young's modulus of SRG0 (129 kPa) is almost half that of PLG0 (240 kPa) and SRG0 can be stretched to 100% strain without failure, whereas PLG0 fails near 35% strain. The Young's modulus of SRG0 is initially recovered by approximately 75% when bonded by SRGlue (95 kPa), and it increases by 15% when bonded by the stiffer PLGlue (149 kPa). All of the bonded gels yield and continue extending at a lower modulus, except PLG0 with SRGlue which did not form a stable bond. SRG0 yields at 2% strain to a modulus of 42 kPa and extends to 17% strain when bonded by SRGlue, while it yields at 19% strain and extends to 27% strain when bonded by PLGlue. The ability of PLGlue to recover the modulus of SRG0 outperforms even that of PLG0, the modulus of which is initially recovered by only 33% (78 kPa) and yields to 29 kPa at 14% strain until failure occurs at 30% strain.

The cut-and-paste strategy opens the door to various macroscopic reconfigurations of slide-ring materials (Figure 4c). For example, the slide-ring adhesive is strong enough to withstand the large volume reductions of the highly acetylated SRG3 gels in hot water. We cut, interlocked, and re-bonded two toroidal SRG0 gels into a Hopf link to demonstrate that the cut-and-paste strategy may also be employed to create topologically non-trivial gels that would be challenging to prepare in conventional molds. We also showed that chemically differentiated gels (SRG0 and SRG3) can be bonded together into hybrid gels with spatially segregated domains of chemical functionality. When this hybrid hydrogel was thermally actuated, the SRG0 domains collapsed to a greater extent than their intact counterparts, indicating that the hydrophobic HMDI crosslinking agent can diffuse beyond the surface of the gel and react with CD rings in its internal network.

4 Conclusions

We have demonstrated two post-synthetic modifications of slide-ring gels that leverage the reactivity of free hydroxyl groups in crosslinked polyrotaxanes derived from PEG and α-CD, as well as fixed-crosslink gels derived from pullulan. By varying the concentration of Ac_2O in a swollen organogel, the degree of acetylation can be varied at a fixed crosslink density, with simplified removal of impurities in the product by solvent washing. The gels stiffen upon solvent exchange into water and the corresponding hydrogels undergo temperature-responsive changes in transparency, volume, and softness that can be controlled by the degree of acetylation. The LCST behavior, which is apparent to the naked eye, is accompanied by a dramatic drop in modulus, which is reversible at low acetylation and becomes irreversible at higher acetylation ratios. WAXS data of freeze-dried and heat-dried xero-

gels indicate that the thermo-responsive microstructural changes that occur in solution influence the microstructural outcomes of drying. We also demonstrated slide-ring and pullulan adhesives that enable a cut-and-paste approach to bonding separate slide-ring organogels together. The utility of the cut-and-paste procedure has been demonstrated in the form of hydrogel actuators and topological linking of gels at the macroscopic level. We envision that these simple post-synthetic modification protocols can assist researchers in prototyping and re-configuring slide-ring gels for various applications and devices.

Conflicts of interest

The authors declare no conflict of interest.

Acknowledgements

This work was supported by funding from the College of Engineering and Applied Science at the University of Colorado Boulder and the National Science Foundation (Award No. 2023179). The authors gratefully acknowledge the Soft Materials Research Center for help with the X-ray studies, as well as Ashray Parameswar and Professor Andrew Goodwin for assistance with freeze drying.

Notes and references

1 Y. Okumura and K. Ito, *Adv. Mater.*, 2001, **13**, 485–487.
2 K. Ito, *Polymer*, 2012, **44**, 38–41.
3 A. Bin Imran, K. Esaki, H. Gotoh, T. Seki, K. Ito, Y. Sakai and Y. Takeoka, *Nat. Commun.*, 2014, **5**, 5124.
4 K. Ohtsuka and C. Zhao, *Polymer International*, 2018, **67**, 1112–1117.
5 H. Fujita, T. Ooya, M. Kurisawa, H. Mori, M. Terano and N. Yui, *Macromol. Rapid Commun.*, 1996, **17**, 509–515.
6 H. Fujita, T. Ooya and N. Yui, *Macromolecules*, 1999, **32**, 2534–2541.
7 T. Ikeda, N. Watabe, T. Ooya and N. Yui, *Macromol. Chem. Phys.*, 2001, **202**, 1338–1344.
8 H. S. Choi, S. C. Lee, K. Yamamoto and N. Yui, *Macromolecules*, 2005, **38**, 9878–9881.
9 H. S. Choi, A. Hirasawa, T. Ooya, D. Kajihara, T. Hohsaka and N. Yui, *ChemPhysChem*, 2006, **7**, 1671–1673.
10 T. Sakai, H. Murayama, S. Nagano, Y. Takeoka, M. Kidowaki, K. Ito and T. Seki, *Adv. Mater.*, 2007, **19**, 2023–2025.
11 K. Karaky, C. Brochon, G. Schlatter and G. Hadziioannou, *Soft Matter*, 2008, **4**, 1165–1168.
12 A. B. Imran, T. Seki, K. Ito and Y. Takeoka, *Macromolecules*, 2010, **43**, 1975–1980.
13 H. Zhou, Y. Wang, Z. Zheng, X. Ding and Y. Peng, *Chem. Commun.*, 2014, **50**, 6372–6374.
14 Y. Takashima, Y. Hayashi, M. Osaki, F. Kaneko, H. Yamaguchi and A. Harada, *Macromolecules*, 2018, **51**, 4688–4693.
15 A. Harada and M. Kamachi, *J. Chem. Soc., Chem. Commun.*, 1990, 1322–1323.
16 A. Harada and M. Kamachi, *Macromolecules*, 1990, **23**, 2821–2823.
17 A. Harada, J. Li and M. Kamachi, *Nature*, 1992, **356**, 325–327.
18 S. Choi, T.-W. Kwon, A. Coskun and J. W. Choi, *Science*, 2017, **357**, 279–283.
19 D. J. Yoo, A. Elabd, S. Choi, Y. Cho, J. Kim, S. J. Lee, S. H. Choi, T.-W. Kwon, K. Char, K. J. Kim, A. Coskun and J. W. Choi, *Adv. Mater.*, 2019, **31**, 1901645–10.
20 Y. Cho, J. Kim, A. Elabd, S. Choi, K. Park, T.-W. Kwon, J. Lee, K. Char, A. Coskun and J. W. Choi, *Adv. Mater.*, 2019, **31**, 1905048–9.
21 N. Sugihara, Y. Tominaga, T. Shimomura and K. Ito, *Electrochim. Acta*, 2015, **169**, 433–439.
22 N. Sugihara, K. Nishimura, H. Nishino, S. Kanehashi, K. Mayumi, Y. Tominaga, T. Shimomura and K. Ito, *Electrochim. Acta*, 2017, **229**, 166–172.
23 Y.-C. Lin, K. Ito and H. Yokoyama, *Polymer*, 2018, **136**, 121–127.
24 L. Imholt, D. Dong, D. Bedrov, I. Cekic-Laskovic, M. Winter and G. Brunklaus, *ACS Macro Lett.*, 2018, **7**, 881–885.
25 L. Imholt, T. S. Dörr, P. Zhang, L. Ibing, I. Cekic-Laskovic, M. Winter and G. Brunklaus, *J. Power Sources*, 2019, **409**, 148–158.
26 Q. Lin, X. Hou and C. Ke, *Angew. Chem., Int. Ed.*, 2017, **129**, 4523–4528.
27 Q. Lin, L. Li, M. Tang, X. Hou and C. Ke, *J. Mater. Chem. C*, 2018, **50**, 161–5.
28 Q. Lin, M. Tang and C. Ke, *Polym. Chem.*, 2020, **11**, 304–308.
29 M. Nakahata, S. Mori, Y. Takashima, H. Yamaguchi and A. Harada, *Chem*, 2016, **1**, 766–775.
30 J. Seo, S. W. Moon, H. Kang, B.-H. Choi and J.-H. Seo, *ACS Appl. Mater. Interfaces*, 2019, **11**, 1–12.
31 J. Wang, W. Wang, X. Geng, T. Nishi, X. Zhao and L. Zhang, *RSC Adv.*, 2018, **8**, 36172–36180.
32 J. Wang, X. Geng, W. Wang, L. Zhang, X. Zhao and T. Nishi, *J. Appl. Polym. Sci.*, 2018, **136**, 47188–7.
33 K. Kato, T. Mizusawa, H. Yokoyama and K. Ito, *J. Phys. Chem. Lett.*, 2015, **6**, 4043–4048.
34 K. Kato, T. Mizusawa, H. Yokoyama and K. Ito, *J. Phys. Chem. C*, 2017, **121**, 1861–1869.
35 K. Kato, K. Nemoto, K. Mayumi, H. Yokoyama and K. Ito, *ACS Appl. Mater. Interfaces*, 2017, **9**, 32436–32440.
36 K. Kato, A. Ohara, K. Michishio and K. Ito, *Macromolecules*, 2020, **53**, 8910–8917.
37 C. Katsuno, A. Konda, K. Urayama, T. Takigawa, M. Kidowaki and K. Ito, *Adv. Mater.*, 2013, **25**, 4636–4640.
38 S. Tan, Q. Fu, J. M. P. Scofield, J. Kim, P. A. Gurr, K. Ladewig, A. Blencowe and G. G. Qiao, *J. Mater. Chem. A*, 2015, **3**, 14876–14886.
39 N. Yui, T. Ooya, T. Kawashima, Y. Saito, I. Tamai, Y. Sai and A. Tsuji, *Bioconjugate Chem.*, 2002, **13**, 582–587.
40 M. Eguchi, T. Ooya and N. Yui, *J. Controlled Release*, 2004, **96**, 301–307.
41 H. Utsunomiya, R. Katoono, N. Yui, T. Sugiura, Y. Kubo, Y. Kato and A. Tsuji, *Macromol. Biosci.*, 2008, **8**, 665–669.

42 J.-H. Seo, S. Kakinoki, Y. Inoue, T. Yamaoka, K. Ishihara and N. Yui, *Soft Matter*, 2012, **8**, 5477.

43 J.-H. Seo, S. Kakinoki, Y. Inoue, K. Nam, T. Yamaoka, K. Ishihara, A. Kishida and N. Yui, *Biomaterials*, 2013, **34**, 3206–3214.

44 J.-H. Seo, S. Kakinoki, Y. Inoue, T. Yamaoka, K. Ishihara and N. Yui, *J. Am. Chem. Soc.*, 2013, **135**, 5513–5516.

45 Y. Arisaka, A. Tonegawa, A. Tamura and N. Yui, *J. Appl. Polym. Sci.*, 2020, **138**, 49706–9.

46 R. Sekiya-Aoyama, Y. Arisaka, M. Hakariya, H. Masuda, T. Iwata, T. Yoda and N. Yui, *Biomater. Sci.*, 2021, –.

47 J. W. Fredy, J. Scelle, A. Guenet, E. Morel, S. Adam de Beaumais, M. Ménand, V. Marvaud, C. S. Bonnet, E. Tóth, M. Sollogoub, G. Vives and B. Hasenknopf, *Chem. – Eur. J.*, 2014, **20**, 10915–10920.

48 T. Ooya, H. Mori, M. Terano and N. Yui, *Macromol. Rapid Commun.*, 1995, **16**, 259–263.

49 T. Ooya and N. Yui, *J. Controlled Release*, 1999, **58**, 251–269.

50 T. Ooya, K. Arizono and N. Yui, *Polym. Adv. Technol.*, 2000, **11**, 642–651.

51 C. Moon, Y. M. Kwon, W. K. Lee, Y. J. Park, L.-C. Chang and V. C. Yang, *J. Biomed. Mater. Res.*, 2008, **84A**, 238–246.

52 N. Yui, R. Katoono and A. Yamashita, *Adv. Polym. Sci.*, 2009, **222**, 55–77.

53 L. Jiang, Z.-m. Gao, L. Ye, A.-y. Zhang and Z.-g. Feng, *Polymer*, 2013, **54**, 5188–5198.

54 R.-J. Jiang, B. Yang, Z.-K. Liu, Y.-L. Zhao, X.-L. Liao, J. Yang, C.-Z. Gao, F. Wang and B. Han, *Carbohydr. Res.*, 2013, **380**, 149–155.

55 Y. Kang, X.-M. Zhang, S. Zhang, L.-S. Ding and B.-j. Li, *Polym. Chem.*, 2015, **6**, 2098–2107.

56 S. Bai, X. Zhang, X. Ma, J. Chen, Q. Chen, X. Shi, M. Hou, P. Xue, Y. Kang and Z. Xu, *Biomater. Sci.*, 2018, **6**, 3126–3138.

57 G. Yu, Z. Yang, X. Fu, B. C. Yung, J. Yang, Z. Mao, L. Shao, B. Hua, Y. Liu, F. Zhang, Q. Fan, S. Wang, O. Jacobson, A. Jin, C. Gao, X. Tang, F. Huang and X. Chen, *Nat. Commun.*, 2018, 1–13.

58 T. Ooya, H. S. Choi, A. Yamashita, N. Yui, Y. Sugaya, A. Kano, A. Maruyama, H. Akita, R. Ito, K. Kogure and H. Harashima, *J. Am. Chem. Soc.*, 2006, **128**, 3852–3853.

59 A. Yamashita, N. Yui, T. Ooya, A. Kano, A. Maruyama, H. Akita, K. Kogure and H. Harashima, *Nat. Protoc.*, 2006, **1**, 2861–2869.

60 A. Yamashita, D. Kanda, R. Katoono, N. Yui, T. Ooya, A. Maruyama, H. Akita, K. Kogure and H. Harashima, *J. Controlled Release*, 2008, **131**, 137–144.

61 Y. Yamada, T. Nomura, H. Harashima, A. Yamashita, R. Katoono and N. Yui, *Biol. Pharm. Bull.*, 2010, **33**, 1218–1222.

62 Y. Yamada, T. Nomura, H. Harashima, A. Yamashita and N. Yui, *Biomaterials*, 2012, **33**, 3952–3958.

63 A. Tamura and N. Yui, *J. Mater. Chem. B*, 2013, **1**, 3535–3544.

64 A. Tamura and N. Yui, *Biomaterials*, 2013, **34**, 2480–2491.

65 V. D. Badwaik, E. Aicart, Y. A. Mondjinou, M. A. Johnson, V. D. Bowman and D. H. Thompson, *Biomaterials*, 2016, **84**, 86–98.

66 R. Ardeleanu, A. I. Dascalu, A. Neamtu, D. Peptanariu, C. M. Uritu, S. S. Maier, A. Nicolescu, B. C. Simionescu, M. Barboiu and M. Pinteala, *Polym. Chem.*, 2018, **9**, 845–859.

67 Y. Ji, X. Liu, M. Huang, J. Jiang, Y.-P. Liao, Q. Liu, C. H. Chang, H. Liao, J. Lu, X. Wang, M. J. Spencer and H. Meng, *Biomaterials*, 2019, **192**, 416–428.

68 S. B. Ghodke, J. N. Parkar, A. R. Deshpande, P. P. Dandekar and R. D. Jain, *ACS Appl. Bio Mater.*, 2020, **3**, 7500–7514.

69 A. Tamura, G. Ikeda, J.-H. Seo, K. Tsuchiya, H. Yajima, Y. Sasaki, K. Akiyoshi and N. Yui, *Sci. Rep.*, 2013, **3**, 2252.

70 A. Tamura, G. Ikeda, K. Nishida and N. Yui, *Macromol. Biosci.*, 2015, **15**, 1134–1145.

71 R. C. Ball, M. Doi, S. F. Edwards and M. Warner, *Polymer*, 1981, **22**, 1010–1018.

72 P.-G. de Gennes, *Physica A*, 1999, **271**, 231–237.

73 K. Ito, *Polymer*, 2007, **39**, 489–499.

74 M. B. Pinson, E. M. Sevick and D. R. M. Williams, *Macromolecules*, 2013, **46**, 4191–4197.

75 K. Kato, T. Yasuda and K. Ito, *Macromolecules*, 2013, **46**, 310–316.

76 K. Kato, T. Yasuda and K. Ito, *Polymer*, 2014, **55**, 2614–2619.

77 T. Müller, J.-U. Sommer and M. Lang, *Soft Matter*, 2019, **15**, 3671–3679.

78 F. J. Vernerey and S. Lamont, *J. Mech. Phys. Solids*, 2021, **146**, 104212.

79 K. Mayumi, M. Tezuka, A. Bando and K. Ito, *Soft Matter*, 2012, **8**, 8179–8183.

80 K. Kato, Y. Ikeda and K. Ito, *ACS Macro Lett.*, 2019, **8**, 700–704.

81 N. Murata, A. Konda, K. Urayama, T. Takigawa, M. Kidowaki and K. Ito, *Macromolecules*, 2009, **42**, 8485–8491.

82 Y. Bitoh, N. Akuzawa, K. Urayama, T. Takigawa, M. Kidowaki and K. Ito, *Macromolecules*, 2011, **44**, 8661–8667.

83 K. Kato and K. Ito, *Soft Matter*, 2011, **7**, 8737–8740.

84 C. Liu, H. Kadono, K. Mayumi, K. Kato, H. Yokoyama and K. Ito, *ACS Macro Lett.*, 2017, **6**, 1409–1413.

85 C. Liu, K. Mayumi, K. Hayashi, L. Jiang, H. Yokoyama and K. Ito, *J. Electrochem. Soc.*, 2019, **166**, B3143–B3147.

86 C. Liu, H. Kadono, H. Yokoyama, K. Mayumi and K. Ito, *Polymer*, 2019, **181**, 121782.

87 E. Caló and V. V. Khutoryanskiy, *Eur. Polym. J.*, 2015, **65**, 252–267.

88 Y. Shinohara, K. Kayashima, Y. Okumura, C. Zhao, K. Ito and Y. Amemiya, *Macromolecules*, 2006, **39**, 7386–7391.

89 G. Fleury, G. Schlatter, C. Brochon and G. Hadziioannou, *Adv. Mater.*, 2006, **18**, 2847–2851.

90 G. Fleury, G. Schlatter, C. Brochon, C. Travelet, A. Lapp, P. Lindner and G. Hadziioannou, *Macromolecules*, 2007, **40**, 535–543.

91 S. Loethen, T. Ooya, H. S. Choi, N. Yui and D. H. Thompson,

Biomacromolecules, 2006, **7**, 2501–2506.
92 K. Kato, H. Komatsu and K. Ito, *Macromolecules*, 2010, **43**, 8799–8804.
93 H. Sun, J. Han and C. Gao, *Polymer*, 2012, **53**, 2884–2889.
94 T. Ooya and N. Yui, *J. Biomater. Sci., Polym. Ed.*, 1997, **8**, 437–455.
95 T. Ooya, M. Akutsu, Y. Kumashiro and N. Yui, *Sci. Technol. Adv. Mater.*, 2005, **6**, 447–451.
96 J. Araki, *J. Polym. Sci., Part A: Polym. Chem.*, 2011, **49**, 2199–2209.
97 J. Araki and K. Ito, *J. Polym. Sci., Part A: Polym. Chem.*, 2005, **44**, 532–538.
98 M. Kidowaki, T. Nakajima, J. Araki, A. Inomata, H. Ishibashi and K. Ito, *Macromolecules*, 2007, **40**, 6859–6862.
99 J. Zhang, L. Zhang, S. Li, C. Yin, C. Li, W. Wu and X. Jiang, *ACS Biomater. Sci. Eng.*, 2017, **4**, 1963–1968.
100 J. Araki, K. Kagaya and K. Ohkawa, *Biomacromolecules*, 2009, **10**, 1947–1954.
101 J. Araki, K. Ohkawa, Y. Uchida and Y. Murakami, *J. Polym. Sci., Part A: Polym. Chem.*, 2011, **50**, 488–494.
102 T. Ooya, M. Eguchi, A. Ozaki and N. Yui, *Int. J. Pharm. (Amsterdam, Neth.)*, 2002, **242**, 47–54.
103 J. Araki, T. Kataoka and K. Ito, *Soft Matter*, 2008, **4**, 245–249.
104 T. Ooya, T. Kawashima and N. Yui, *Biotechnol. Bioprocess Eng.*, 2001, **6**, 293–300.
105 A. B. Imran, T. Seki, T. Kataoka, M. Kidowaki, K. Ito and Y. Takeoka, *Chem. Commun.*, 2008, **25**, 5227–3.
106 B. Pérès, N. Richardeau, N. Jarroux, P. Guégan and L. Auvray, *Biomacromolecules*, 2008, **9**, 2007–2013.
107 J. Araki and K. Ito, *J. Polym. Sci., Part A: Polym. Chem.*, 2006, **44**, 6312–6323.
108 A. Bando, R. Kasahara, K. Kayashima, Y. Okumura, K. Kato, Y. Sakai, H. Yokoyama, Y. Shinohara, Y. Amemiya and K. Ito, *Polymers*, 2016, **8**, 217–15.
109 M. Inutsuka, K. Inoue, Y. Hayashi, A. Inomata, Y. Sakai, H. Yokoyama and K. Ito, *Polymer*, 2015, **59**, 10–15.
110 H. Hyun and N. Yui, *Macromol. Rapid Commun.*, 2010, **32**, 326–331.
111 S. Y. Zheng, C. Liu, L. Jiang, J. Lin, J. Qian, K. Mayumi, Z. L. Wu, K. Ito and Q. Zheng, *Macromolecules*, 2019, **52**, 6748–6755.
112 L. Feng, S. S. Jia, Y. Chen and Y. Liu, *Chem. – Eur. J.*, 2020, **26**, 14080–14084.
113 J. Araki and N. Sainou, *Polymer*, 2015, **74**, 133–143.
114 L. Jiang, C. Liu, K. Mayumi, K. Kato, H. Yokoyama and K. Ito, *Chem. Mater.*, 2018, **30**, 5013–5019.
115 H. Murayama, A. B. Imran, S. Nagano, T. Seki, M. Kidowaki, K. Ito and Y. Takeoka, *Macromolecules*, 2008, **41**, 1808–1814.
116 K. Ogata, M. Kidowaki, K. Ito and K. Terashima, *J. Photopolym. Sci. Tech.*, 2010, **23**, 535–540.
117 J. Araki, C. Zhao and K. Ito, *Macromolecules*, 2005, **38**, 7524–7527.
118 M. Kidowaki, C. Zhao, T. Kataoka and K. Ito, *Chem. Commun.*, 2006, 4102–4103.
119 T. Karino, Y. Okumura, C. Zhao, M. Kidowaki, T. Kataoka, K. Ito and M. Shibayama, *Macromolecules*, 2006, **39**, 9435–9440.
120 T. Kataoka, M. Kidowaki, C. Zhao, H. Minamikawa, T. Shimizu and K. Ito, *J. Phys. Chem. C*, 2006, **110**, 24377–24383.
121 A. Tonegawa, A. Tamura and N. Yui, *ACS Macro Lett.*, 2019, **8**, 826–834.
122 A. Tonegawa, A. Tamura and N. Yui, *Macromol. Rapid Commun.*, 2020, **41**, 2000322–6.
123 H. G. Schild, *Prog. Polym. Sci.*, 1992, **17**, 163–249.
124 T. Murakami, B. V. K. J. Schmidt, H. R. Brown and C. J. Hawker, *J. Polym. Sci., Part A: Polym. Chem.*, 2017, **55**, 1156–1165.
125 G. Paul, J. A. Huwaldt and S. Steinhorst, *Plot Digitizer, v 2.6.9*, https://sourceforge.net/projects/plotdigitizer/, 2020.
126 Y. Zhao, Y. Cao, Y. Yang and C. Wu, *Macromolecules*, 2003, **36**, 855–859.
127 K. Kato, K. Ito and T. Hoshino, *J. Phys. Chem. Lett.*, 2020, **11**, 6201–6205.
128 B. D. Fairbanks, S. P. Singh, C. N. Bowman and K. S. Anseth, *Macromolecules*, 2011, **44**, 2444–2450.
129 Z. Wei, J. H. Yang, J. Zhou, F. Xu, M. Zrínyi, P. H. Dussault, Y. Osada and Y. M. Chen, *Chem. Soc. Rev.*, 2014, **43**, 8114–8131.
130 D. L. Taylor and M. in het Panhuis, *Adv. Mater.*, 2016, **28**, 9060–9093.